CHAPTER 2

BACKGROUND THEORIES

This chapter contains details on the description of necessary principles that relate to the research i.e. crystal structures, x-ray interactions with atoms, x-ray absorption spectroscopy, x-ray absorption near edge structure calculation, extended x-ray absorption fine structure equation and density functional theory.

2.1 Crystal structures

In crystallography, crystal structures can be primarily divided into 7 crystal systems which are cubic, tetragonal, orthorhombic, rhombohedral, hexagonal, monoclinic and triclinic. Further, these can be further classified into 32 point groups according to their crystallographic symmetry. However, only 21 point groups do not have a center of symmetry. Of these 21 point groups, 20 point groups correspond to materials which have the properties that an applied mechanical stress (on the materials) produces an electric field or on the other hand an electric field produces a mechanical stress. Such materials can be referred to as "piezoelectric" materials. In addition, these 20 piezoelectric materials can be subdivided into 10 sub-materials that have spontaneous polarization or electrical polarity. These polar groups have the property that the change in temperature induces an electric field. Such materials are called "pyroelectric" materials. A subset of these pyroelectric can have their spontaneous polarization reversed or enhanced by the application of a high enough electric field. This subset of the pyroelectric is the "ferroelectric" materials. The classification of the crystal structures showing the division into piezoelectric, pyroelectric and ferroelectric can be shown in Figure 2.1.

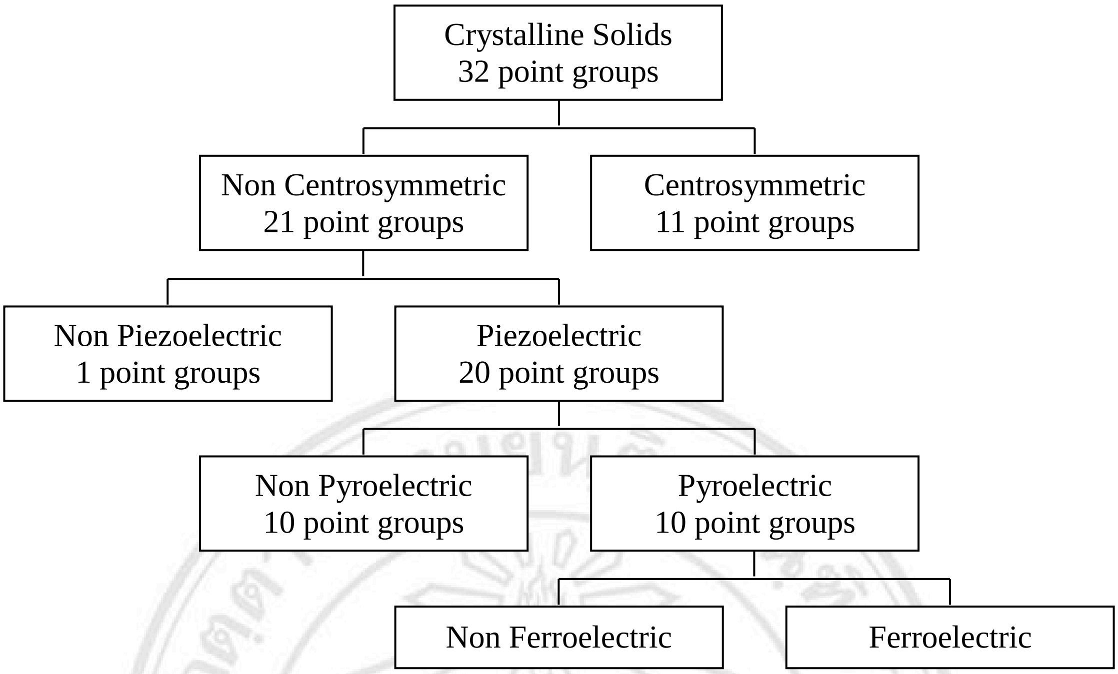

Figure 2.1 The classification of crystal structures showing the division into piezoelectric, pyroelectric and ferroelectric materials (modified from [5]).

There are many crystal structures associated with different physical properties of oxide compounds. For example, cubic, tetragonal, hexagonal and monoclinic structures for mechanical oxides, octahedron, rutile and anatase structures for optical oxides, and perovsike and ferrite structures for electrical oxides. Nevertheless, this thesis will focus only on electrical and magnetic oxide materials having mostly perovskite structure with a generic formula, i.e. ABO_3. This perovskite structure has a primitive cubic structure with A-cation (alkali, alkaline earth and rare earth ion) in the middle of the cube, B-cation on the corner of the cube, and the O-anion (commonly oxygen) at the center of the cubic faces as shown in Figure 2.2.

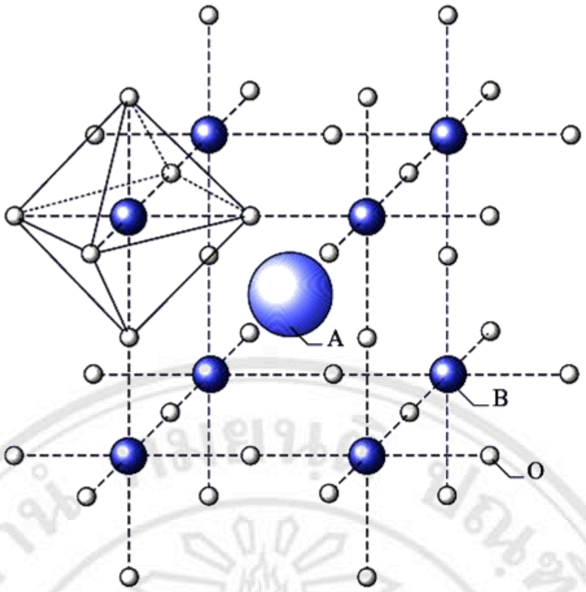

Figure 2.2 Perovskite structure [6].

2.2 X-ray interactions with atoms

The discovery of x-ray by W.C. Roentgen in 1895 (Nobel laureate in 1901) opened up new frontiers in the investigation of matter since x-ray has wavelengths approximating to atomic distances in materials. Further, being discovered by M.V. Laue in 1912 (Nobel laurate in 1914), x-ray absorbed in matter could generate the emission of electrons with characteristic energies. However, x-ray is electromagnetic radiation having wavelength ranges from about 0.1 Å to 100 Å corresponding to energy ranges from about 120 eV to 120 keV (which covers the binding energies of all electrons in most atoms). With these wavelength and energy regions, x-ray can be absorbed by most matters which result two important x-ray interactions i.e. x-ray absorption and x-ray scattering as the following.

2.2.1 X-ray absorption

In x-ray absorption process, the binding energy of bound electrons in the core shell (e.g. *K*, *L* and *M* shells) must be less than the energy of the incident x-ray. If the binding energy is greater than the incident x-ray energy, the bound electrons in the core shell will not be absorbed x-ray and will not be perturbed from their states. If the binding energy is less than the incident x-ray energy, the bound electrons in the core shell will be excited by the absorbed x-ray to higher empty energy state above the Fermi energy, which gives rise to photoelectron ejected from the atom as shown in Figure 2.3(a). After that, there appears empty energy state in the core shell, and electron in the higher energy shell steps down to fill the core hole shell which emits fluorescence x-ray. The energy of fluorescence x-ray is equal to the difference of electron energies between the unoccupied higher state and the occupied core state as shown in Figure 2.3(b). Additionally, other electrons in higher energy shell may be excited by fluorescence x-ray, and ejected from the atom. This phenomenon is called auger electron emission as shown in Figure 2.3(c).

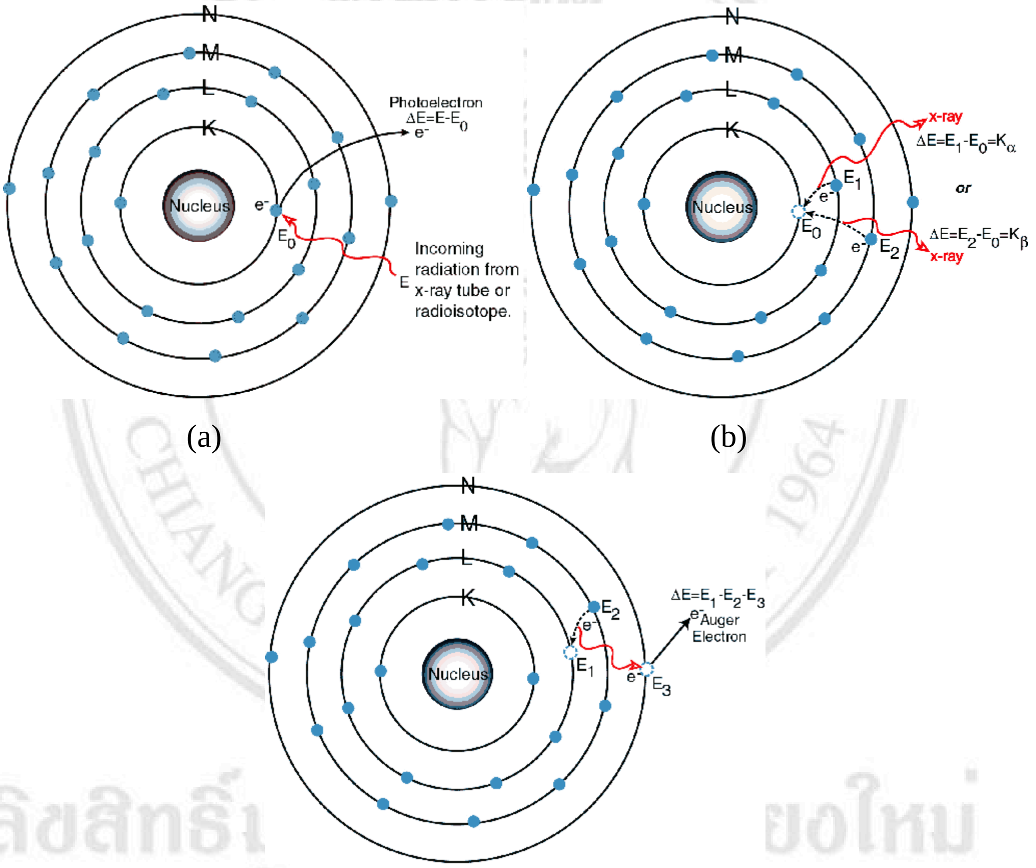

(a)

(b)

(c)

Figure 2.3 Schematic diagram of (a) x-ray absorption, (b) fluorescence x-ray emission and (c) auger electron emission when incident x-ray is applied on electrons in an atom.

2.2.2 X-ray scattering

There are two types of x-ray scattering i.e. elastic scattering (Rayleigh scattering / coherent scattering) and inelastic scattering (Compton scattering / incoherent scattering). In Rayleigh scattering, x-ray is scattered by bound electrons but electrons are neither excited nor ionized. The x-ray loses negligible fraction of energies. The wavelength of incident x-ray is almost equal to that of scattered x-ray. In Compton scattering, x-ray is scattered by bound electrons and electrons are excited but not ionized. The x-ray loses some parts of energies. It is possible that the final x-ray have a different energy from the initial x-ray without the emission of electrons. The wavelength of incident x-ray is less than that of scattered x-ray. The schematic diagram for both mentioned x-ray scatterings is shown in Figure 2.4.

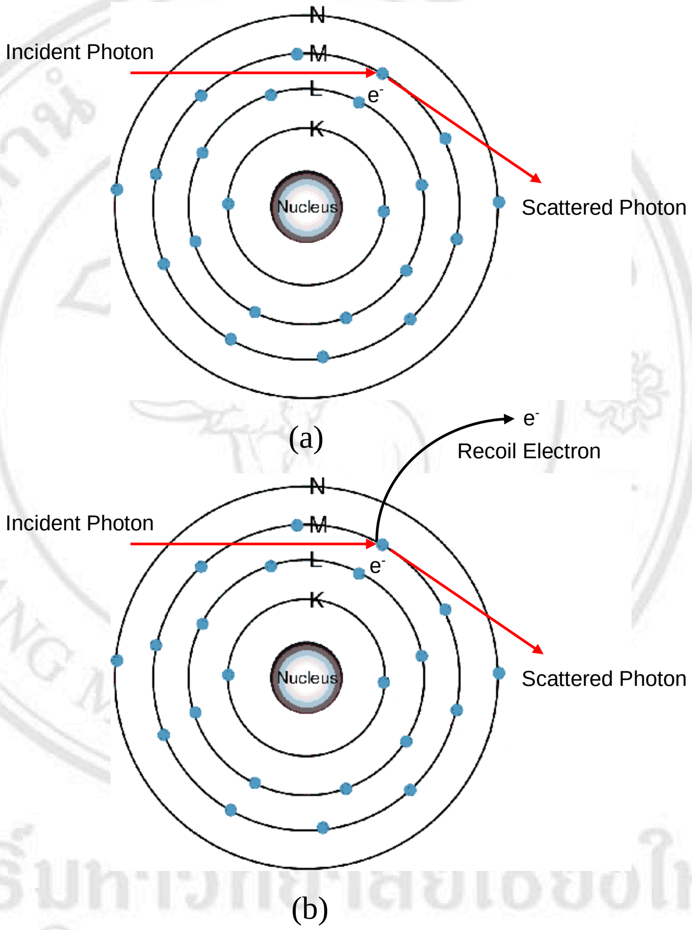

Figure 2.4 Schematic diagram of (a) Rayleigh scattering and (b) Compton scattering when incident x-ray is applied on electrons in an atom.

The strength of an x-ray interaction such as absorption and scattering can be quantified in terms of the total cross section σ_{tot}, which has units of area, and generally is a function of energy. The special unit of area, “barn” (10^{-24} m^2), is used because barns are a convenient size of nuclear, where nuclear dimensions are only a few femtometers.

Typically, the total photon cross section σ_{tot} comprises the contributions of several processes i.e. photon absorption (photoelectron) $\sigma_{p.e.}$, coherent scattering (Rayleigh scattering) σ_{coh}, incoherent scattering (Compton scattering) σ_{incoh}, nuclear absorption (photonuclear, usually followed by emission of a neutron or other particle) σ_{nuc}, pair production (electron field) K_e, pair production (nuclear field) K_n is a function of photon energy as shown in Figure 2.5.

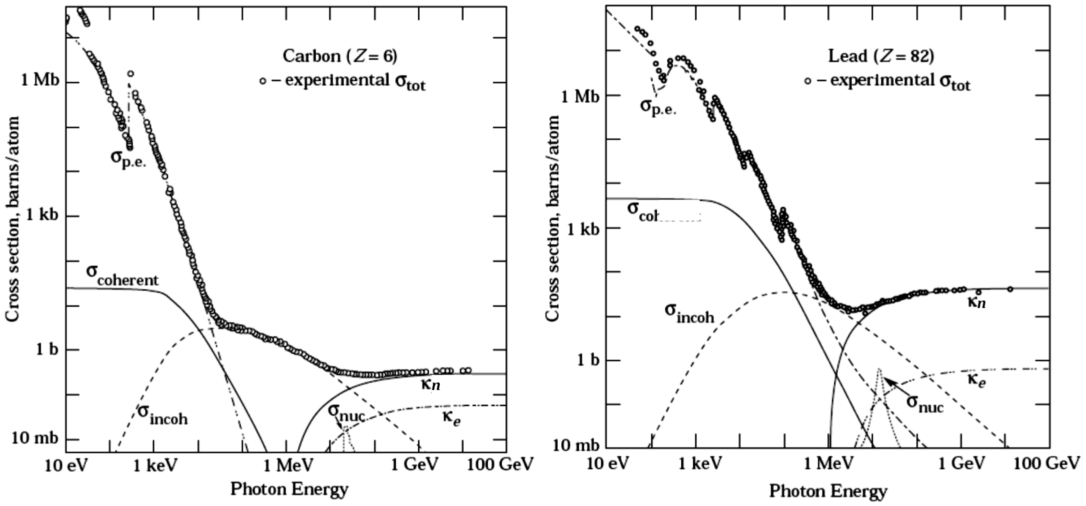

Figure 2.5 The total photon cross section as a function of photon energy in carbon and lead, showing the contributions of different processes at different energies [7].

From Figure 2.5, the total photon cross section comprises the contributions of the photon absorption, coherent scattering, and incoherent scattering, but the photoelectron cross section is dominant in the x-ray energy ranges (from about 1 keV to 1 MeV). Therefore, the total photon cross section is approximately identical to the absorption coefficient μ that can be obtained from x-ray absorption spectroscopy.

2.3 X-ray absorption spectroscopy

X-ray absorption spectroscopy (XAS) is a powerful experimental technique for determining local structure surrounding an absorbing atom in both ordered and disordered materials such as crystals, amorphous, glasses, films, membranes, liquids, solutions and molecular gases, which used in a wide variety of disciplines such as physics, chemistry, biology, medicine, engineering, environmental science, material science, and geology. This technique is a measure of the probability that photon is absorbed by the sample as a function of its energy. From x-ray absorption process, x-ray absorption spectrum can be detected in three modes i.e. transmission mode, fluorescence mode and electron yield mode. In transmission mode, x-ray absorption spectrum is obtained from the ratio of x-ray intensities before and after x-ray is passed the sample. Since x-ray is electromagnetic wave, being absorbed by the homogeneous material, the absorption coefficient μ is described by the Lambert-Beer's law [8] i.e.

$$I = I_0 e^{-\mu x}, \tag{2.1}$$

where I_0 is the incident x-ray intensity and I is the transmit x-ray intensity after the x-ray propagated the distance of x inside the sample. In fluorescence mode, is obtained from the ratio of the incident x-ray intensity I_0 and the fluorescence x-ray intensity I_f that are emitted after x-ray absorption event. Generally, the absorption coefficient μ smoothly decreases as the x-ray energy increases (approximately varies as $1/E^3$) i.e. the x-ray become more penetrating in the sample. The characteristic feature of the absorption coefficient is the x-ray absorption edges i.e. the minimum photon energy that is large enough to excite a bound electron into the continuum for each sub-shell (binding energy). In the x-ray absorption edge region, the absorption coefficient sharply increases. The emitted electron is called photoelectron. If the incident photon has higher energy, the photoelectron's wave can propagated and scattered on neighboring atoms around absorbing atom. To probe local structure around absorbing atom with accuracy, x-ray should be absorbed by electron in core shell (e.g. K, L and M shells), which having the large interval of binding energies and the long range of photon energies to determine absorbing atom local structure without the x-ray absorption edges overlapping (see example for tungsten atom in Table 2.1).

Table 2.1 Electron binding energies of tungsten atom (Z = 74) [9].

N	L	J	Number of electrons	X-ray label	Energy (eV)
1	0	$\frac{1}{2}$	2	K	-69,525
2	0	$\frac{1}{2}$	2	L_{I}	-12,100
	1	$\frac{1}{2}$	2	L_{II}	-11,544
	1	$\frac{3}{2}$	4	L_{III}	-10,207
3	0	$\frac{1}{2}$	2	M_{I}	-2,819
	1	$\frac{1}{2}$	2	M_{II}	-2,575
	1	$\frac{3}{2}$	4	M_{III}	-2,281
	2	$\frac{3}{2}$	4	M_{IV}	-1,872
	2	$\frac{5}{2}$	6	M_{V}	-1,809
4	0	$\frac{1}{2}$	2	N_{I}	-595
	1	$\frac{1}{2}$	2	N_{II}	-492
	1	$\frac{3}{2}$	4	N_{III}	-425
	2	$\frac{3}{2}$	4	N_{IV}	-259
	2	$\frac{5}{2}$	6	N_{V}	-245
	3	$\frac{5}{2}, \frac{7}{2}$	14	$N_{\text{VI,VII}}$	-35
5	0	$\frac{1}{2}$	2	O_{I}	-77
	1	$\frac{1}{2}$	2	O_{II}	-47
	1	$\frac{3}{2}$	4	O_{III}	-36
	2	$\frac{3}{2}, \frac{5}{2}$	4	$O_{\text{IV,V}}$	-6

Traditionally, x-ray absorption spectrum can be divided into two regions according to photon energies as shown in Figure 2.6. The low energy region covers photon energy up to about 40 eV above the x-ray absorption edge is called the x-ray absorption near-edge structure (XANES). In this photon energy region, the core electron is excited to the unoccupied state, so that the shape of the absorption edge depends on the density of states just above the Fermi level. Therefore, the oxidation state and geometry of an absorbing atom affect XANES spectrum. Additionally, this low energy range shows characteristic features for different oxidation state of the absorbing atom. The absorption edge in the XANES usually shifts to higher energy with the oxidation state of the absorbing atom increasing. This is due to that the radial distribution of valence electrons charge could screen the nuclear charge in the nucleus. As a consequence, the core electrons get less screened and stronger attracted to the nucleus so it does cost larger energy to bring these core electrons to an excited state.

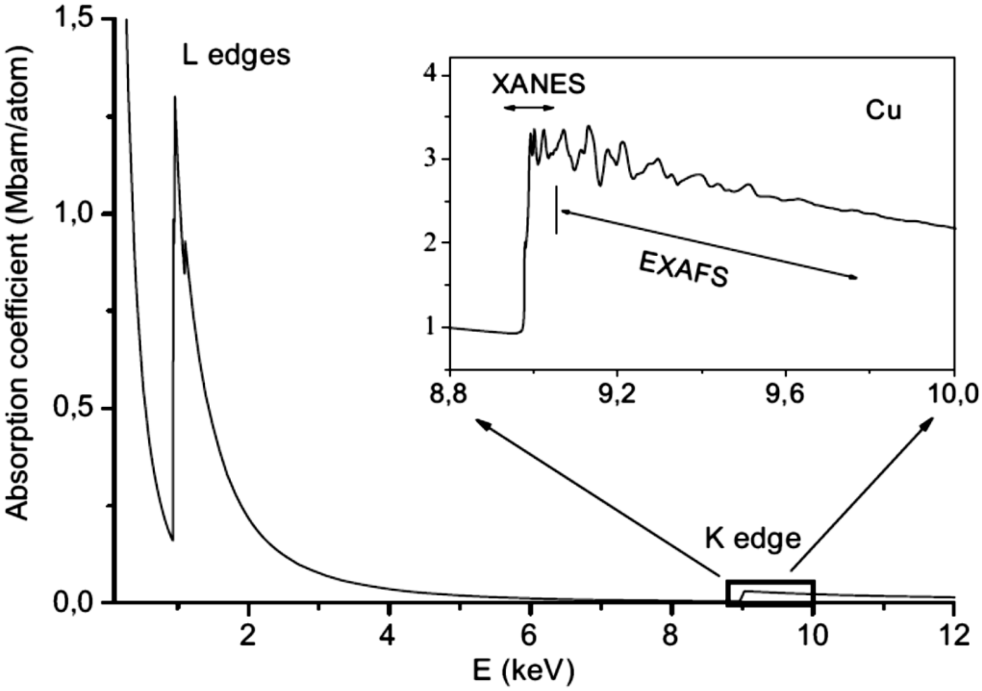

Figure 2.6 X-ray absorption spectroscopy (XAS) of Cu presenting the *L*-edge and *K*-edge regions. The inset shows an amplified view of the x-ray absorption near-edge structure (XANES) and the extended x-ray absorption fine structure (EXAFS) of the *K*-edge region [10].

The high energy region covering photon energy up to about 1000 eV above above the x-ray absorption edge is called the extended x-ray absorption fine structure (EXAFS). In this energy range, the photon energy is far above the ionization threshold and the photoelectron can be considered as an outgoing spherical wave as shown in Figure 2.7. The neighboring atoms around absorbing atom are scattered this photoelectron wave, and there exists interference between the outgoing wave and the scattering waves if they meet at a same place. This leads to the final XAS spectrum which is indeed the superposition of the outgoing and the scattered waves. For constructive interference, the signal is enhanced leading to a maximum in the EXAFS oscillation. For destructive interference, the signal is suppressed leading to a minimum in the EXAFS oscillation. EXAFS can then be used in the investigation of neighboring atoms around absorbing atom.

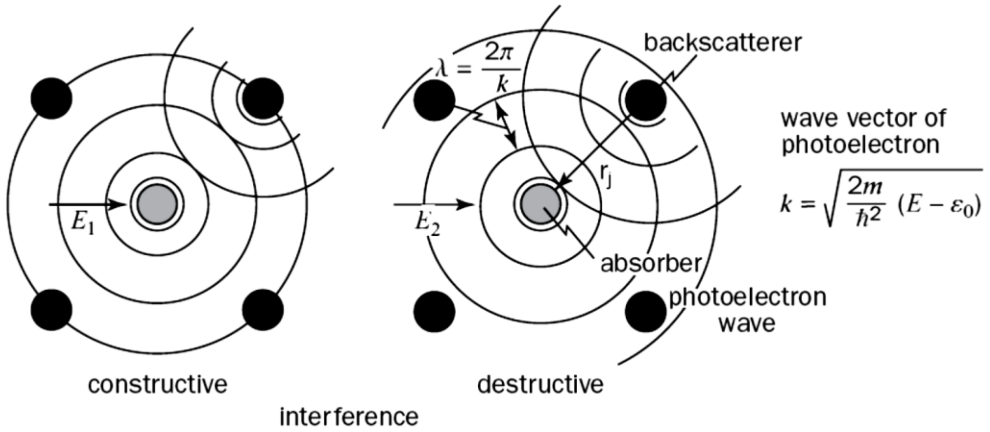

Figure 2.7 Schematic diagram of the outgoing and the backscattering photoelectron wave leading to the EXAFS oscillations. E is the absorbed photon energy and E_0 is the core level binding energy [11].

2.3.1 XANES theory

The x-ray absorption spectroscopy is intrinsically quantum mechanical phenomenon. The absorption coefficient μ measured by x-ray absorption spectroscopy experimental relates to the transition rate of photoelectron from initial core state $|i\rangle$ to final state $|f\rangle$ above Fermi energy. The transition rate is determined within single electron and dipole approximation by Fermi's golden rule [12] as

$$\mu \propto \sum_f |< f\,|\,\hat{\varepsilon}\cdot\vec{r}\,|\,i >|^2\, \delta(E_f - E_i - \hbar\omega), \qquad (2.2)$$

where $\hat{\varepsilon}\cdot\vec{r}$ is the dipole operator for the incident electromagnetic wave on atoms and electrons. Therefore, the absorption coefficient μ is non-zero only above the Fermi energy i.e. only for incident photon energies that are large enough to promote the core electron into an unfilled state.

The Hamiltonian of core state is $H_0 = -(1/2)\nabla^2 + V$. The Hamiltonian of excited state is $H = H_0 + V_{ch} + \sum(E)$ including a core potential V_{ch} and a complex energy dependent quasi-particle self-energy $\sum(E)$. The single electron Green's function can then be written as $G = 1/(E - H + i\zeta)$, where ζ is the intrinsic broadening due to the final core hole lifetime. The sum over final states and the energy conserving delta function together can be compactly written in term of Green's function $(-1/\pi)\,\mathrm{Im}\,G = \sum_f |\, f\rangle \delta(E_f - E_i - \hbar\omega)\langle f\,|$. The absorption function $\mu(E)$ is rewritten

$$\mu(E) \propto (-1/\pi)\,\mathrm{Im}\langle i\,|\,\hat{\varepsilon}\cdot\vec{r}\,' G(\vec{r},\vec{r}\,';E)\hat{\varepsilon}\cdot\vec{r}\,|\,i\rangle. \tag{2.3}$$

The Green's function defined above is the full single electron propagator in the presence of the scattering potential. G can be expressed in a series by the Dyson equation

$$G = G^0 + G^0 t G^0 + G^0 t G^0 t G^0 + \ldots, \tag{2.4}$$

where $G^0 = 1/(E - H_0 + i\zeta)$ is the free electron propagator, describes the propagation of an electron from one angular momentum state in one atom to another atom and another angular momentum state and t is the atomic scattering matrix, describes the scattering from each site. The successive terms are the successive orders of scattering contributing to the dipole matrix element. The second term contains the description of all single scattering events wherein an electron propagates to the scatterer, scatters from it, and propagates back to the first atom. The third term describes all events involving the scattering from two atoms before propagating back to the first atom. The higher order terms have similar interpretations. All propagations starting at the central atom, that atom which absorbed the photon and emitted a photoelectron, are calculated.

$$G = G_c + \sum_{i\neq 0} G_c t_i G_c + \sum_{i\neq j} G_c t_i G^0_{i,j} t_j G_c + \ldots, \tag{2.5}$$

$$G = G_c + \sum_{\substack{\text{all possible}\\ \text{paths}}} G^{\Gamma} \tag{2.6}$$

where G_c is the free electron propagator between the central atom and some neighboring atom and $G^0_{i,j}$ is the propagator between the atom *i* and *j*. the sum are over all possible scattering geometries of each order of scattering. The terms excluded from the sums are those for the propagation of an electron from some atom back to itself. The superscript Γ denotes some scattering path. All possible scattering geometries Γ

within some cluster of neighboring atoms around the absorbing atom are calculated.

The full multiple scattering fine structure can be extracted from $G^{\Gamma}_{L_f,L_f}$ given as

$$\chi(E) = \mathrm{Im}\left(\exp(2i\delta_{l_f})\frac{1}{2l_f+1}\sum_m G_{L.L'}(\rho,E) \right)\times \qquad (2.7)$$
$$\delta(R-R_{central})\delta(R'-R_{central})\delta(l-l_f)\delta(l'-l_f)\delta(m-m'),$$

where l_f is the final state angular momentum, R_0 is the central atom, δ_{l_f} is the central atom phase shift for angular momentum l_f. The Dirac delta function restrict this trace to the central atom and to the angular momentum of the photoelectron final state l_f.

The absorption function $\mu(E)$ contains both the embedded atom background $\mu_0(E)$ and the absorption fine structure $\chi(E)$ i.e.

$$\mu(E) = \mu_0(E)(1+\chi(E)). \qquad (2.8)$$

The embedded atom background $\mu_0(E)$ is computed by directly evaluating the integral in Eq. (2.2) using the initial core state and the final state of the embedded atom i.e. the neutral atom within the muffin tin potential. The full multiple scattering absorption function μ_{FMS} is computed from μ_0 and Eq. (2.7).

2.3.2 EXAFS equation

As previously mentioned, the absorption fine structure $\chi(E)$ can be rewritten by the quantity

$$\chi(E) = \frac{\mu(E)-\mu_0(E)}{\Delta\mu_0(E)}, \qquad (2.9)$$

where $\Delta\mu_0(E)$ is the absorption edge jump. As previously mentioned, the scattering of the outgoing photoelectron wave from the neighboring atoms affects the amplitude of the photoelectron, which eventually results in the oscillation of the linear absorption coefficient with changing x-ray energy. From this qualitative picture an expression to calculate the EXAFS can be deduced. Conventionally, the EXAFS oscillations are often defined with respect to the photoelectron wave number *k*

$$k = \sqrt{\frac{2m}{\hbar^2}(E - E_0)}, \tag{2.10}$$

where E_0 is the binding energy of the core electron that is excited and $E = \hbar\omega$ is the energy of the absorbed photon.

The outgoing photoelectron can be described by a spherical wave with amplitude which is proportional to $\exp(ikr)/r$, where k is wavenumber of photoelectron. The neighboring atoms scatter the incoming spherical wave into the outgoing spherical wave and this wave is proportional to the amplitude of the incident wave and the backscattering amplitude $F(k)$, which depends on the type of backscattering atom. The amplitude of the backscattered wave at the origin is proportional to $F(k)\exp(i2kr)/r^2$.

The photoelectron is not moving in a constant potential, a phase shift $\delta(k)$ has to be added to this expression to account for the interaction of the electron with the varying potential of the absorber atom and of the backscatter atom. It must be distinguished between the phase shift of the absorbing atom $\delta_a(k)$ and the backscattering atom $\delta_b(k)$. $\delta(k)$ is the sum of both phase shifts, but the phase shift of the absorber atom $\delta_a(k)$ has to be counted twice in this sum, hence, $\delta(k) = 2\delta_a(k) - l\pi + \delta_b(k)$, where $l = 1$ for *K*-edges according to the dipole selection rules. Thus, $\chi_j(k)$ is given by

$$\chi_j(k) = F_j(k)\frac{e^{i(2kr_j+\delta_j(k))} + e^{-i(2kr_j+\delta_j(k))}}{2r_j^2}, \tag{2.11}$$

or

$$\chi_j(k) = F_j(k)\frac{\sin(2kr_j + \delta_j(k))}{r_j^2}. \tag{2.12}$$

In condensed matter, the absorber atom has in general more than one next nearest neighbour and, therefore, Equation 2.12 must be summed over the scattering contribution of all neighbours. Atoms at the same radial distance and of the same element contribute to the same components of the EXAFS signal. This group of atoms is called a (coordination) shell. The coordination number of each shell is N_j and the sum in $\chi(k)$ runs over all shells *j*.

The distance between the absorber and the backscatterers in each shell might not be identical due to structural disorder and moreover the atoms vibrate due to thermal excitations which also influences the distance between the absorber atom and the backscatterer. Thus, the contributions from atoms in one shell will not be exactly in phase. If the disorder is small and has a Gaussian distribution around the average distance *R*, the dephasing can be taken into account for by a factor $\exp(-2k^2\sigma_j^2)$ and $\sigma_j^2 = \langle[\vec{r}_j \cdot (\vec{u}_j - \vec{u}_0)]^2\rangle$ is the mean square average of the difference of displacements $(\vec{u}_j - \vec{u}_0)$ of the backscatterer *j* and the absorber along the equilibrium bond direction $\vec{r}_j$. The term is often referred to as EXAFS Debye-Waller factor but it should be noticed that this factor is not equivalent to the Debye-Waller factor in x-ray diffraction $\sigma_{\mathrm{XRD}}^2 = \langle(\vec{r}_j - \vec{u}_j)^2\rangle$, which is the mean square displacement. Usually the EXAFS Debye-Waller factor is smaller as compared to the XRD Debye-Waller factor as only the vibrations relative to the absorbing atom are taken into account for and for example long wavelength phonons will not contribute to the EXAFS Debye-Waller factor, since the two atoms (absorber and backscatterer) are too close to each other and the contribution to the difference $(\vec{u}_j - \vec{u}_0)$ is negligible.

The last effect is the lifetime τ_0 of the excited photoelectron states, which depends on the time it takes until the core hole is filled by another electron and on the lifetime of the photoelectron itself. Within the lifetime of the photoelectron state (e.g., $\tau_0 = 2\times10^{-15}$ s for a Cu 1*s* electron) the outgoing and the backscattered wave are coherent and thus both waves can interfere. This means that the number of shells contributing to the spectrum is limited by the fact that the outgoing and the backscattered wave must be coherent and, therefore, the finite lifetime of the photoelectron state damps the oscillations due to backscattering from neighbouring atoms at higher distances. Usually it is expected that shells, which are further apart than 10 Å from the absorber, are not visible in the spectrum. The damping factor equals $\exp(-2r_j/\lambda(k))$ and $\lambda(k)$ is called the mean free path. The mean free path depends only little on the element. So finally, the following expression is obtained to describe the EXAFS oscillations $\chi(k)$

$$\chi(k) = \sum_j \frac{N_j S_0^2 F_j(k) \exp(-2r_j / \lambda(k)) \exp(-2k^2\sigma_j^2)}{kr_j^2} \sin(2kr_j + \delta_j(k)). \qquad (2.13)$$

The amplitude reduction term (or passive electron reduction factor) S_0^2 accounts for the relaxation of all other electrons in the absorber atom due to the creation of the core hole. Although S_0^2 is weakly energy dependent, it is usually approximated by a constant. The amplitude reduction term differs for different elements and the values range from 0.6 < S_0^2 < 1.0.

Parameters in Eq. 2.13 include N_j, the number of equivalent routes in the j^{th} scattering path; r_j, the haft mean distance of the j^{th} scattering path; S_0^2, an average amplitude reduction factor where its value is the percent weight of the main excitation channel with respect to all possible excitation channels (its value is usually in the range 0.6-1.0); $F_j(k)$, the backscattering amplitude of the neighbor atoms in j^{th} scattering path; and $\delta_j(k)$, the electronic phase shift due to the atomic potentials. The exponential term $\exp(-2k^2\sigma_j^2)$ takes into account of fluctuations of distances due to a structural and/or thermal disorder, under the assumption of small displacements and Gaussian distributions of distances. The exponential term $\exp(-2r_j / \lambda(k))$ takes into account of finite elastic mean free paths of photoelectrons $\lambda(k)$.

The scattering properties of the neighboring atom i.e. the backscattering amplitude $F_j(k)$, the phase shift of the absorbing atom and its backscatter $\delta_j(k)$, and the elastic mean free paths of photoelectrons $\lambda(k)$ can be calculated from single and multiple scattering theories, which depends on the type of backscatter. The important parameters are distance to the neighboring atom (R_j), coordination number of neighboring atom (N_j) and mean-square disorder of neighbor distance (σ_j^2) which can be determined. The scattering amplitude $F_j(k)$ and phase-shift $\delta_j(k)$ depend on atomic number, so that XAS is therefore sensitive to atomic number Z of neighboring atom. These scattering properties can be accurately calculated and used in the EXAFS modeling. The sum over paths in the EXAFS equation includes many scattering paths of absorbing atoms, and can also include multiple-scattering paths, in which the photoelectron scatters from more than one atom before returning to the central atom (e.g. see Figure 2.8). From sum over paths in the EXAFS equation, the predicted important parameters will be accepted when the EXAFS from modeling matches with that of the experiment.

(a) single scattering path (b) double scattering path (c) triple scattering path

Figure 2.8 Schematic diagrams of the different scattering paths when the scattering angle at the absorbing atom is 180°.

One of the most convenient ways to analyze EXAFS results is to use the Fourier transform on the data, and express the transformed results in *r*-space. This is as the Fourier transformations plays an essential role in the analysis in interpreting EXAFS data to obtain the system local structure. Specifically, the peaks (with high magnitude) of the Fourier transform of the EXAFS spectrum can be related to the atomic distances in the material investigated. Therefore the principles of Fourier transformations necessary to understand and perform the analysis of EXAFS data are discussed. The Fourier transform $\chi(r)$ of the fine structure $\chi(k)$ in the EXAFS analysis is defined by:

$$\chi(r) = \frac{1}{\sqrt{2\pi}} \int_{k_{\min}}^{k_{\max}} k^n \chi(k) w(k) e^{i2kr} dk, \tag{2.14}$$

where $w(k)$ is the window function gradually increases from zero at the beginning of the data range (Δk) and gradually decreases to zero at the end of the data range. The k range used in the transformation is given by $k_{\min}$ and $k_{\max}$. As can be seen, the fine structure $\chi(k)$ is weighted by a factor k^n prior to the transformation and n usually equals 1, 2 or 3, since the oscillations are usually decayed with higher wave numbers k. Therefore, the weighting factor is used to compensate for any effect which diminishes the amplitude with increasing k such as the $1/k$ dependence of the fine structure and the characteristic behavior of the backscattering amplitude function. The weighting factor n should be chosen such that the amplitude of $k^n\chi(k)$ is maintained over the k-range of the data used in the transformation. Since the noise usually increases at higher wave numbers *k*, it has to be taken into account that a larger weighting factor *n* also amplifies the noise contributions especially at high *k*-values compared to those of the low *k*-values, and therefore it might be necessary to choose a small weighting factor when analyzing data with a low signal-to-noise ratio. The Fourier transform of EXAFS oscillation from modeling and experiment can also be compared in *r*-space to extract the local structure information.

Usually, the above mentioned parameters are varied for optimization (to fit the results to those of the experiments). Generally, these parameters are not necessarily independent of each other for different scattering paths, and the number of parameters grows rapidly with the number of scattering paths included in the fit. The number of parameters N_{idp} that can be reliably determined in a fit is limited by the data range Δk and ΔR according to the Nyquist theorem [13],

$$N_{\mathrm{idp}} = \frac{2\Delta k \Delta R}{\pi}. \tag{2.15}$$

In the equation, N_{idp} gives an estimate of the maximum number of independent parameters. If many different paths have to be taken into account to simulate the measured EXAFS spectrum, the number of parameters to be refined in the fit can easily exceed the number of independent parameters. In addition, the statistical parameter to determine the fit quality is the *R*-factor i.e.

$$R = \frac{\sum_{i=1}^{N} [\chi(R_i)_{\mathrm{thy}} - \chi(R_i)_{\mathrm{exp}}]^2}{\sum_{i=1}^{N} [\chi(R_i)_{\mathrm{exp}}]^2}, \tag{2.16}$$

Typically, *R*-factors below 0.02 indicate a good fit [14].

2.4 Density functional theory

The density functional theory is a phenomenally successful approach to finding quantum solution to the fundamental equation that describes the quantum behavior of materials. Schrödinger's equation is defined by

$$\left[-\frac{\hbar^2}{2m}\sum_{i=1}^{N}\nabla_i^2+\sum_{i=1}^{N}V(r_i)+\frac{e^2}{4\pi\varepsilon_0}\sum_{i=1}^{N}\sum_{j>i}^{N}\frac{1}{r_{ij}}\right]\psi=E\psi, \tag{2.17}$$

where $-\frac{\hbar^2}{2m}\sum_{i=1}^{N}\nabla_i^2$ is the kinetic energy of each electron, $\sum_{i=1}^{N}V(r_i)$ is the interaction energy between electron and nuclei, and $\sum_{i=1}^{N}\sum_{j>i}^{N}\frac{1}{r_{ij}}$ is the interaction energy between pair of electrons. ψ is the many-electron wave function, which is the function of each of spatial coordinates of each of N electrons $\psi=\psi(r_1,...,r_N)$, and E is the ground state energy of electrons. Although Schrödinger's equation solving can be viewed as the fundamental problem of quantum mechanics, the electron wave function in particular set of coordinates cannot be directly observed. The quantity that can be measured is the probability that N electrons are in particular set of coordinates $r_1,...,r_N$, which relate to the density of electrons at a particular position in space. The density of electrons $n(r)$ can be written in the summation over all the probability that an electron with individual electron wave function $\psi_i(r)$ is located at position r as

$$n(r)=2\sum_{i=1}^{N}\psi_i^*(r)\psi_i(r). \tag{2.18}$$

Schrödinger's equation solving of the ground state energy is the unique functional of the electron density. Hohenberg-Kohn equation can be given as

$$\left[-\frac{\hbar^2}{2m}\sum_{i=1}^{N}\nabla_i^2+\int V(r)n(r)dr+\frac{e^2}{2}\iint\frac{n(r)n(r')}{|r-r'|}drdr'\right]\psi=E\psi, \tag{2.19}$$

where $-\frac{\hbar^2}{2m}\sum_{i=1}^{N}\nabla_i^2$ is the kinetic energy of electron, $\int v(r)n(r)dr$ is the interaction energy between electron and nuclei, and $\frac{e^2}{2}\iint\frac{n(r)n(r')}{|r-r'|}drdr'$ is the interaction energy between pairs of electrons. The electron density can be expressed that involves solving a set of equations which each equation only involves a single-electron. The Kohn-Sham equation can be given as

$$\left[-\frac{\hbar^2}{2m}\nabla^2 + V(r) + V_H(r) + V_{xc}(r)\right]\psi_i(r) = \varepsilon_i \psi_i(r). \tag{2.20}$$

The solution of Kohn-Sham equation is single-electron wave function $\psi_i(r)$, where $V(r)$ is potential defines the intraction between an electron and nuclei, $V_H(r)$ is Hartree potential defines the coulomb repulsion between pairs of electrons has the form

$$v_H(r) = e^2 \int \frac{n(r')}{|r - r'|} d^3r', \tag{2.21}$$

$V_{xc}(r)$ is potential defines exchange and correlation contributions to single-electron equations has the form

$$v_{xc}(r) = \frac{\delta E_{xc}(r)}{\delta n(r)}. \tag{2.22}$$